Cement and Concrete Research 38 (2008) 1015–1025

Contents lists available at ScienceDirect

Cement and Concrete Research

journal homepage: http://ees.elsevier.com/CEMCON/default.asp

Microstructural modifications in Portland cement concrete due to forced ionic migration tests. Study by impedance spectroscopy

I. Sánchez [a], X.R. Nóvoa [b], G. de Vera [a], M.A. Climent [a,*]

[a] Departament d'Enginyeria de la Construcció, Obres Públiques i Infraestructura Urbana, Universitat d'Alacant, Ap. Correus 99, 03080, Alacant/Alicante, Spain
[b] Departamento de Enxeñeria Química, E.T.S.E.I., Universidade de Vigo, Spain

ARTICLE INFO

Article history:
Received 24 February 2006
Accepted 11 March 2008

Keywords:
Impedance spectroscopy
Ionic migration
Diffusion
Chloride
Microstructure

ABSTRACT

The forced migration test has been used during the last decades as an accelerated and useful method for determining the resistance of concrete to chloride ingress. Furthermore it allows to determine transport parameters of chloride ions through porous materials. The application of electric fields seems to introduce variations in the microstructure of concrete. In this work these variations have been studied using the impedance spectroscopy technique in the high frequency region (1 kHz–1 MHz). The results show that the dielectric response of concrete is also strongly modified during the migration experiments. The variations of the dielectric parameters during the migration tests can be explained in terms of modifications of the microstructure of concrete. The observed modifications are in good agreement with the results of mercury porosimetry analysis.

1. Introduction

Chloride ions are responsible of many of the corrosion problems of steel embedded in reinforced or prestressed concrete [1,2]. These corrosion phenomena lead frequently to early deterioration and eventually to risky situations for the stability of structures. In any case, the economic costs inherent to reparation works are considerable.

The presence of chloride ions (Cl^-) in concrete is due to two main causes: they can be added in the mix components, or they can ingress into concrete from the environment. The addition of Cl^- at the time of mixing is normally due to the use of chloride contaminated components. Some years ago chloride salts were purposefully admixed as hardening accelerators, although this practice has nowadays disappeared. Cast-in chlorides cause variations of the microstructure of cement mortar and concrete, as compared with non-contaminated reference materials. In general terms the pore size distributions are modified and the tortuosity of the porous network is increased when Cl^- are admixed [3,4].

The most frequent situation is the ingress of Cl^- from the environment through the pore paths of concrete. Several ingress mechanisms may operate, depending on the environmental conditions, although the mechanism that has attracted more interest is diffusion, which started to be studied about 30 years ago [5–8]. Big efforts have been made to design test methods of chloride ingress into concrete [9–18]. Some of these methods are aimed only to rank concrete mixes according to their resistance to chloride ingress, which can be very useful when choosing the materials at the design phase of structures. Other methods also intend to determine Cl^- transport parameters, mainly the diffusion coefficient. These parameters can be used, in conjunction with transport models, for service life estimations of new or existing structures [19].

Pure diffusion tests, normally performed with diffusion cells or with Cl^- solution ponding setups, are time consuming and involve big experimental effort for chemical analysis of Cl^- content of many samples. This led quickly to the proposal of forced migration tests, based on the application of electric fields, to speed up the transport of ions through concrete specimens [9]. The experimental conditions in migration tests are somehow similar to those prevailing in electrochemical chloride removal trials. Both steady-state and non steady-state ionic diffusion coefficients can be derived from migration experiments [17]. Even the technique of impedance spectroscopy in the very low frequency range (0.1–11.31 Hz) has been used to determine the Cl^- diffusion coefficient on the basis of the diffusion tail appearing in the impedance spectra [20]. Recently, it has been proposed a new method for determining chloride diffusion coefficients based on impedance measurements of some dielectric parameters in the 100 Hz–40 MHz frequency range [21]. In this last work it has been also studied the modifications of the dielectric response of cement mortar samples during chloride migration trials.

Several researches have shown, mainly by mercury porosimetry (MIP) and scanning electron microscopy (SEM) analyses, that ionic migration through concrete causes changes in its pore size distribution. The main effect being a refinement of the pore structure, i.e. a decrease in the number of large pores and an increase in the number

* Corresponding author.
E-mail address: ma.climent@ua.es (M.A. Climent).

0008-8846/$ – see front matter © 2008 Elsevier Ltd. All rights reserved.
doi:10.1016/j.cemconres.2008.03.012

of small pores [22–24]. Nevertheless, some differences have been found in the microstructure of the concrete regions near the cathode and near the anode after finishing the migration experiments [22,24]. The technique used in the present work to determine modification in concrete microstructure has been impedance spectroscopy (IS).

In recent years it has been shown that impedance spectroscopy is a powerful technique to study the microstructure and mechanic properties of cement paste, mortar and concrete. It is due to the possibility of correlating dielectric and mechanic properties of cementitious materials [25–27].

For the concrete-steel system a complete impedance spectra has been described in a previous work [28]. As stated in that work the dielectric properties appear in the high frequency range (~MHz). The key point in the interpretation of the impedance spectra is the determination of the time constants present in this high frequency range. Initial works in this field considered the presence of only one time constant in the dielectric response range [29–32]. This interpretation led to very high dielectric constant values ($\varepsilon > 10^3$) very far from the typical values found for ceramic materials. The high values obtained were justified introducing a dielectric amplification factor (DAF). A different model, with two time constants in the high frequency loop, was proposed, and the values obtained for the dielectric constant were more reasonable [33,34]. The authors of these latter works also proposed different experimental setups to avoid the physical contact between electrodes and sample, thus eliminating the influence of the sample-electrode interface. Later it has been established, using a numerical technique such as differential impedance analysis, introduced by Stoynov et al. [35], that in the high frequency loop two time constants coexist, one of them associated to the solid phase of the material, while the other corresponds to the electrolyte filling the pores [36]. It has been shown that this technique allows to follow changes in microstructure of cement paste, using quite simple representations. The simplicity of impedance measurements, and the possibility of measuring in situ, whenever it is considered necessary, suggests that this technique is useful to study the modifications produced in concrete microstructure by forced ionic migration.

A recently published work [37], shows the influence of migration on the impedance spectra. However, this study does not intend to study microstructural changes, but proposes a new theoretical study on the influence of the AC electric field on the ionic transfer. The equivalent circuit used for the interpretation of the spectra obtained returns to the concept of DAF, which includes only one time constant [30,31]. The high values obtained for the dielectric parameters may be due to the induction resulting from the leads at the high frequency of the electric signal, aspect mentioned as one of the main problems, but also from the equivalent circuit used to interpret the impedance spectra [37].

The main interest of the present paper is to establish the possibility of using impedance spectroscopy to measure the modifications of microstructure in real time and without perturbing the migration experimental conditions.

2. Experimental setup

Concrete samples were prepared using a Portland cement with limestone filler, CEM II A-L 42.5 R. The water/cement ratio used was 0.5.

Table 1
Composition of concrete

Component	Mass/vol. (kg/m^3)
Cement II A-L 42.5 R	350
Coarse aggregate 6–12 mm Ø	714
Coarse aggregate 4–6 mm Ø	489.5
Sand	662.75
H_2O	175
Plasticizer	1.40

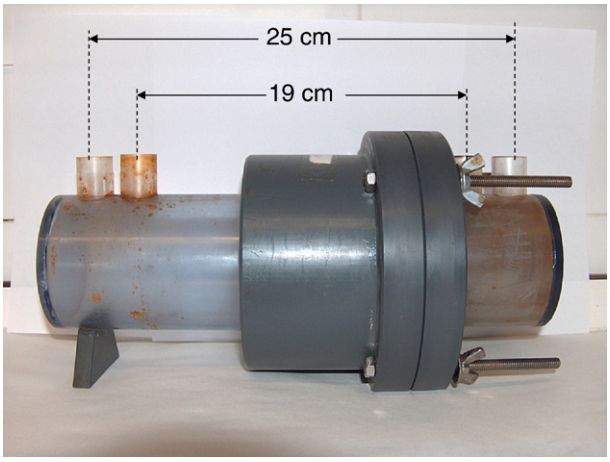

Fig. 1. Photography of the cell used for the migration experiments and the impedance on-line measurements. The driving electrodes are placed at 25 cm distance, and the holes at 19 cm distance are used for the impedance measurements.

The dosage used for concrete preparation is shown in Table 1. The mixture was cast in cylindrical moulds 10 cm in diameter, and 10 cm high. Samples were kept at 100% RH during the hardening time, until starting the experiment. The samples were cut into slices of 1 cm thick. These slices were placed in the cells designed for the forced migration tests.

2.1. Forced migration tests

The forced migration experiments have been performed following essentially an experimental procedure [17], based on monitoring the anolyte conductivity, as this parameter has been shown to be proportional to the chloride content of the anolyte.

The concrete samples were pre-conditioned prior to the migration tests, following a standardized water saturation procedure [38]. A typical cell is shown in Fig. 1. Each electrolyte container has 500 ml of capacity and the concrete sample is placed in between with two silicone rings, leaving exposed circular faces of 6.5 cm diameter for the migration test. The stainless steel electrodes for establishing the driving electric field are placed in the outer apertures of the cell, the distance between them being 25 cm. The inner apertures are used for the electrodes of the impedance measurements.

After checking the absence of liquid leaks between both electrolyte chambers, the catholyte and anolyte chambers are filled with a 1 M NaCl solution and with distilled water, respectively, and the migration experiment begins. The applied driving voltage is 12 V, although the effective potential drop between both sides of the concrete disc is measured periodically by means of two saturated calomel reference electrodes. The conductivity measurements of the anolyte solution were performed each 6 h at the beginning of the experiment, and after the first 60 h the frequency of measurements is set to each 12 h. These measurements were performed with a Crison GLP31 conductimeter (Barcelona, Spain), with automatic compensation of the readings to 25 °C standard temperature. Temperature data of the electrolytes were also recorded.

2.2. Impedance spectroscopy measurements

The impedance spectra of the system solutions-concrete disk were obtained using an AUTOLAB potentiostat/galvanostat with PGSTAT30 impedance analyser with input capacitance <8 pF, and the possibility of obtaining the impedance spectra from 10 μHz to 1 MHz. A two-electrode configuration was employed to perform the measurements. Two stainless steel rods (Ø=4 mm) were placed in the inner apertures of the cells, thus having 19 cm distance between them (see Fig. 1). These electrodes were removed after each impedance measurement.

The frequency range of the IS measurements was from 10 Hz to 1 MHz, because this is the range were dielectric properties appear [28]. Even though the input capacity of the measuring equipment is high, the spectra modifications can be adequately recorded, because the value of the input capacity is the same for all the measurements. The obtained impedance spectra were validated using the Kramers–Kronig (K–K) relations, to ensure causality, linearity and stability of the measurements made [39], with satisfactory results.

Measured data were fitted to an equivalent circuit to obtain the parameters of interest in the system. The circuit used in this work, shown in Fig. 2 is based on a previous circuit originally proposed for cement paste [36], but it has been shown to be effective to fit the impedance spectra obtained for cement mortar, just including the aggregates into the solid phase [27], and a modification for samples immersed in solutions has been made recently [21]. The fitting of the measured data to the model proposed is made using a simplex optimization method which is described elsewhere [33,40].

2.3. Mercury intrusion porosimetry

In order to validate the interpretations of the impedance spectroscopy measurements, in terms of microstructural modifications, a classic technique, such as mercury intrusion porosimetry was used for determining the pore structure of selected samples, taken at different spatial locations and times elapsed since the beginning of the migration tests. Even though there are many facts that suggest that this technique is not optimal for the measurement of the pore sizes [41,42], it is widely used to determine pore sizes and distributions.

There has been recently some discussion on the effect that different types of drying have on the MIP measurements [43,44]. In this work samples were vacuum dried for 48 h and then kept in oven at 50 °C. This procedure assures that no structural water is evaporated. With this preparation, the chosen value for the contact angle was 130°. To ensure that samples used for this measurements were representative they were cut off with irregular and random shapes.

The porosimeter employed was an AUTOPORE IV 9500 from Michromeritics. This porosimeter allows pore diameter determination in the range from 5 nm to 0.9 mm. It has to be considered, that as reported by Diamond [41,42], only the dimensions of the pore superficial structure can be detected by MIP, and the irregularities in pore shape cannot be determined. Nevertheless, information on the possible tortuosity of pore network can be obtained from the mercury retained in the sample after the end of the experiment.

After a MIP test, the analysis of the curve plotting the logarithmic differential intrusion volume vs. pore size, shows the size ranges where pores appear. Usually the pores of concrete are classified into the following categories: gel pores (diameters lower than 10 nm); capillary pores (diameters between 10 nm and 1 μm); and pores with diameters larger than 1 μm. This classification is significant from the point of view of concrete durability, since most mass transfer through concrete takes place through the capillary porosity, while gel pores practically do not contribute to transport. Pores larger than 1 μm are associated to air voids, and considered as coarse porosity [45,46].

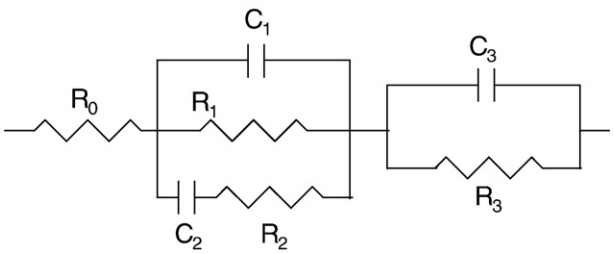

Fig. 2. Equivalent circuit used for the interpretation of the impedance spectroscopy measurements in the high frequency region.

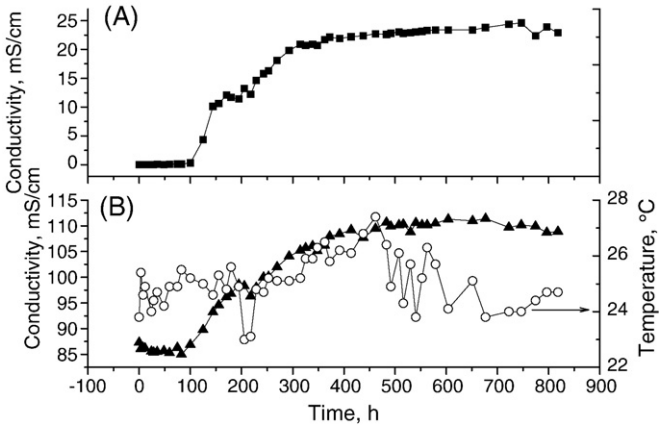

Fig. 3. A. Evolution of the anolyte conductivity with time during the forced migration experiments. B. Evolution of the catholyte conductivity with time during the forced migration experiments (solid triangle) and the temperature of the solutions (open circle).

3. Results

3.1. Forced migration results

After the beginning of the migration experiments the values of conductivity and temperature on both cathodic and anodic sides, and the potential drop between both sides of the sample were measured. Results are depicted in Fig. 3 for conductivity and temperature, and in Fig. 4 for the potential drop. As shown in Fig. 3A, the conductivity of the anolyte is low, (below 1 mS/cm), during the first 100 h of the migration test. After the time-lag the anolyte conductivity increases at an approximately linear rate, indicating that the chloride migration has reached the steady-state, i.e. constant Cl^- flux, and finally the conductivity reaches a constant value of about 25 mS/cm.

Fig. 3B shows that the temperature of the electrolytes remains in the 23 °C to 27 °C range during the migration tests, indicating the absence of an intense heat evolution due to Joule effect [11]. This allows to disregard the possibility of damages of the microstructure due to this side effect. The increase of conductivity of the catholyte, which shows a similar shape pattern as that of the anolyte, is due to the migration of cations from concrete, and to the products of cathodic electrode reactions, where OH^- ions are produced [11]. These ions have a much greater mobility than Cl^-, making the catholyte more conductive.

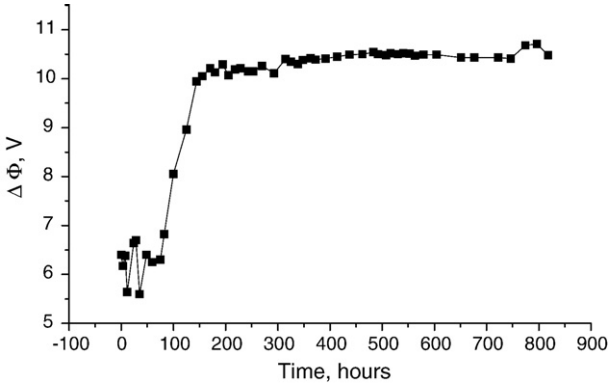

Fig. 4. Changes of the potential drop between the sides of the concrete sample during the forced migration experiment. This potential is measured placing two reference electrodes close to concrete sample.

The values for the non stationary and stationary diffusion coefficients are obtained using Eqs. (1) and (2) [17]:

$$D_{NS} = \frac{2x^2}{\tau v^2}\left[v \coth \frac{v}{2} - 2\right];\ v = \frac{zF\Delta\phi}{RT} \quad (1)$$

$$D_S = \frac{JRTx}{zFC_0\gamma\Delta\phi} \quad (2)$$

where x corresponds to sample thickness, τ is the time-lag, calculated as the time elapsed from the beginning of the test until the conductivity starts to increase in the anodic compartment. $\Delta\Phi$ is the mean value of the potential difference between both sides of the sample. J is the flux of Cl^- ions in steady-state, and it is derived from the slope of the linear part of the conductivity versus time plot. C_0 is the Cl^- initial concentration of the catholyte (1 M). γ corresponds to the Cl^- activity coefficient [47] of the catholyte solution (0.603), and finally T is the average temperature recorded during the experiment. The mean values obtained were $D_{NS} = 1.9 \cdot 10^{-12}$ m^2/s and $D_S = 4.3 \cdot 10^{-12}$ m^2/s.

The driving electrodes corroded significantly during the migration trials, especially the anode. Every time the conductivity was measured, the state of the electrodes was also checked. The possible oxides formed were removed, and the resistivity of the electrode was measured to be sure there was no ohmic drop due to oxide layers. When the electrodes were damaged they were replaced by new ones. The state of a damaged electrode is shown in Fig. 5, where it can be appreciated that the electrode is especially corroded at the bottom.

Finally it has to be pointed out that at the end of the migration experiments the concrete samples appeared covered with a layer of material with the colour of Fe oxides at the anolyte side. This material appeared especially in the cement areas, and not on the aggregate, as can be seen in Fig. 6. MIP and SEM studies, including elementary analysis, were made on samples of these deposits, taken from the concrete surface in contact with the anolyte, after finishing the migration tests. The elemental compositions of these deposits, determined by SEM analysis, are shown in Table 2.

3.2. Impedance spectroscopy results

Impedance spectra of the concrete specimens subjected to migration were measured every 12 or 24 h. These impedance spectra contain both the response of the solutions used in the experiment and the concrete sample. Changes with time in the impedance of the system are due to modifications of the anolyte and the catholyte, as well as changes in the microstructure of the concrete sample. The analysis of the evolution of the impedance spectra may allow understanding the modifications of the concrete microstructure caused by migration. Fig. 7 shows three impedance spectra obtained at different testing times: the initial situation (24 h after the beginning of the experiment), the period where the anolyte conductivity increases linearly (290 h), and the last spectrum shown (600 h), corresponds to the final part of the experiment, where the anolyte conductivity remains approximately constant, see Fig. 3. It is evident from Fig. 7 that important changes occur, being not only a consequence of the variation in the resistance of the electrolytes. It is interesting to note that the low frequency resistance decreases while the anolyte conductivity is increasing, see Figs. 3 and 7, but after some hours of testing the value of this resistance increases.

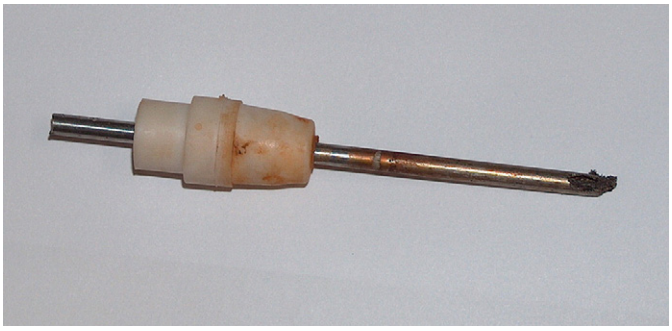

Fig. 5. Driving electrode corroded after some hours of the forced migration experiment. As it can be seen the corrosion phenomena is especially important at the bottom of the electrode.

Fig. 6. Deposits formed on the anodic side of the concrete sample. The deposition of these materials occurs mainly on the cement paste zones, and not over the aggregates.

The impedance spectra measured were successfully fitted to the circuit depicted in Fig. 2 using the procedure explained in Section 2.2. Fig. 8 shows an experimental impedance spectrum and the result of the fitting. Best fitting parameters are also given in the figure caption.

The equation used for the fitting of measured spectra is the following:

$$Z(\omega) = R_0 + \frac{Z_1 \cdot Z_2}{Z_1 + Z_2} + \frac{R_3}{1 + (j\omega R_3 C_3)^{\alpha_3}} \quad (3)$$

$$\text{where } \left(Z_1 = \frac{R_1}{1 + (j\omega R_1 \cdot C_1)^{\alpha_1}} \text{ and } Z_2 = R_2 \cdot (1 + (j\omega R_2 \cdot C_2)^{-\alpha_2})\right) \quad (4)$$

The parameters obtained from the fitting are R_0, R_1, C_1, R_2, C_2, R_3, C_3, α_1, α_2 and α_3. The physical meaning of these parameters has been discussed elsewhere [21,27,36]. R_0 corresponds to the electrolytes at both sides of the concrete sample, between the IS measuring electrodes and the sample. R_1 has been associated to the pores that connect both faces of the concrete sample (percolating pores), while R_2 is related to the pores that do not connect the two sides of the

Table 2
Elemental compositions, determined by SEM analysis, of the deposits formed over the face of concrete sample at the anodic compartment after 410 and 820 h of migration

Element	%	Element	%
O	39.43	O	25.84
Fe	35.78	Fe	58.54
Cr	17.19	Cr	6.41
Cl	4.57	Cl	0.13
Si	0.25	Si	0.25
Ni	1.42	Ni	6.74
Mn	1.37	Mn	1.75
		Ca	0.30
		Al	0.04

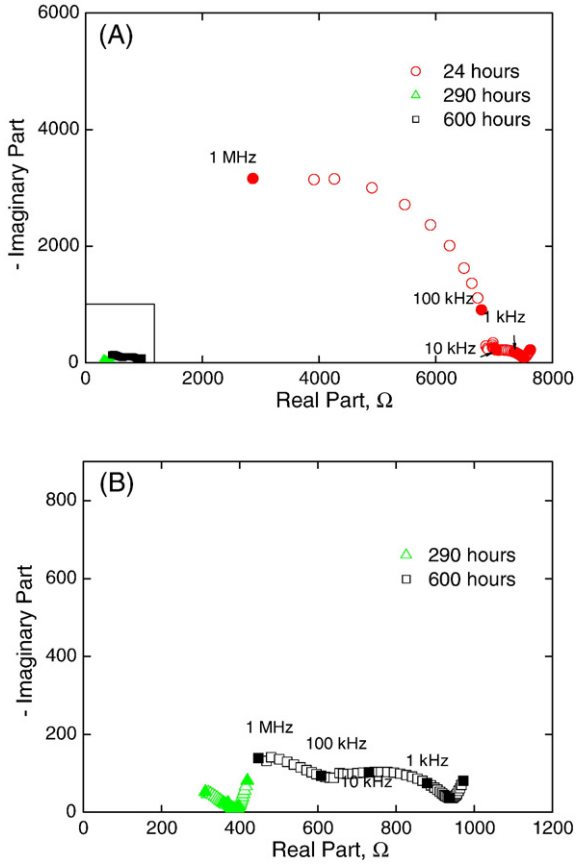

Fig. 7. Evolution of impedance spectra of concrete during the forced migration experiment. Part A depicts the spectra obtained after 24 (circle), 290 (triangle), and 600 h (square) of migration. Part B shows a zoom of the selected area in panel A.

sample (occluded pores). C_1 is a dielectric capacitance, and is related to the solid fraction in the sample, including cement paste and aggregates. C_2 is the capacitance associated to the ionic double layer present at the pore walls-inner concrete electrolyte interface. α_1 and α_2 correspond to Cole–Cole type time constant dispersion factors. R_3, C_3 and α_3 have been associated to the interfaces of the system external electrolytes-concrete [21]. R_3 corresponds to the transfer resistance of these interfaces, and C_3 to the double layer capacitance of both interfaces. α_3 is the dispersion factor associated to this third time constant.

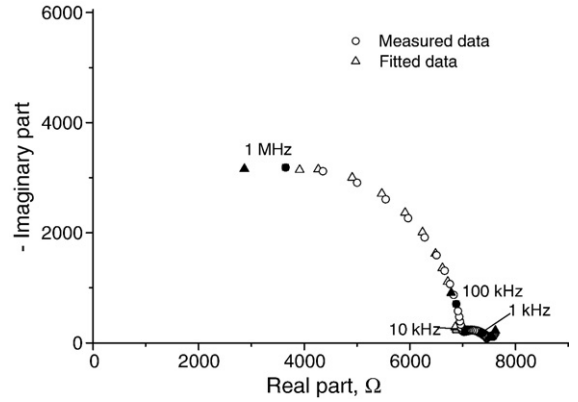

Fig. 8. Measured impedance spectra (circle) and fitted data (triangle) using the equivalent circuit shown in Fig. 2. The best fitting parameters are the following: R_0=649.78 Ω, R_1=6299.1 Ω, C_1=30.60 pF, α_1=0.87, R_2=245.67 Ω, C_2=34.8 pF, α_2=0.86, R_3=728.52 Ω, C_3=0.12 μF, α_3=0.77.

The variations of all these parameters, as a function of ionic migration time are depicted in Figs. 9 and 10. The evolutions of R_1 and R_2 during the migration experiment, (Fig. 9A and B), show clearly decreasing trends during the first 100 h, but afterwards their values tend to increase slightly, and at approximately 400–450 h both resistances show an increase of the slope of the growing lines.

Fig. 9C shows the evolutions of C_1 and C_2, which are very similar for both capacitances. Their value remains approximately constant during the first 200 h of the migration experiment. After this initial stage there is a growing tendency on the value of both capacitances. The value of C_2 increases faster than the value obtained for the capacitance associated to the solid phase (C_1), especially after 500 h.

The evolutions of parameters associated with the external interfaces and electrolytes are depicted in Fig. 10. The resistances R_0

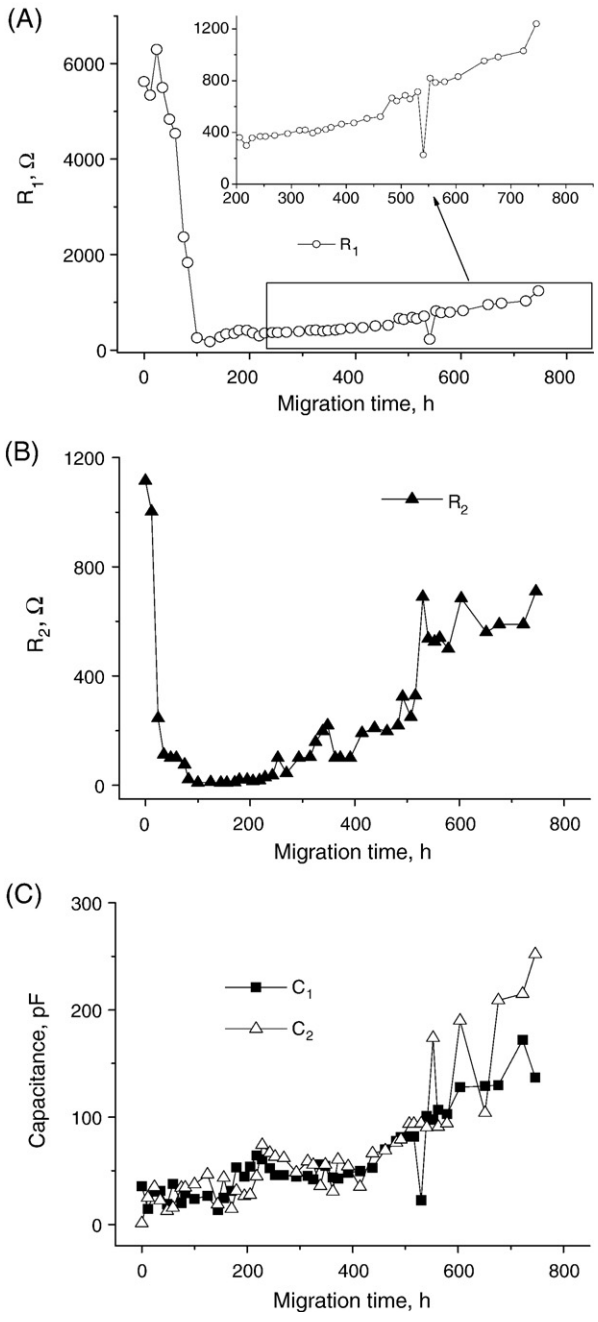

Fig. 9. Evolution of the dielectric parameters corresponding to concrete microstructure, during the migration experiment. See text for details. A) R_1; B) R_2; C) C_1 and C_2.

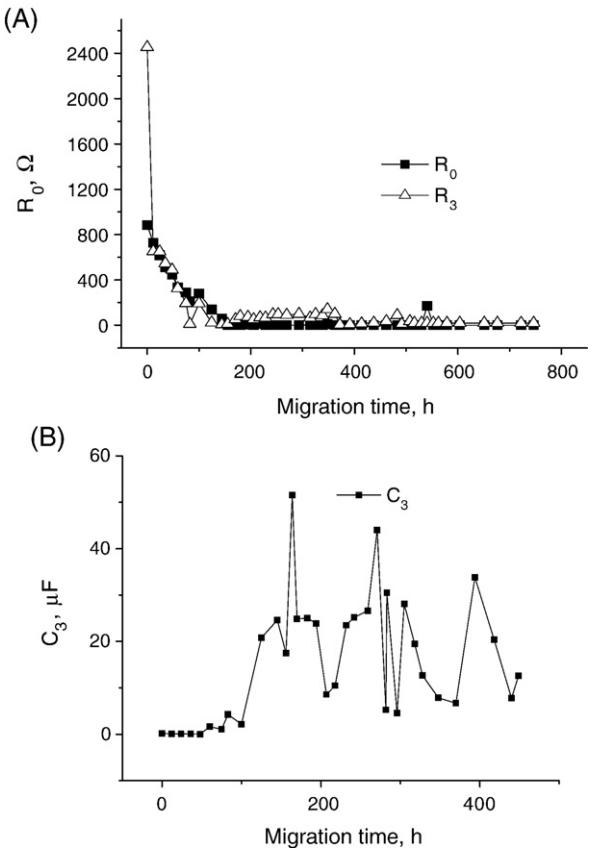

Fig. 10. Evolution of the parameters corresponding to external electrolytes and interfaces concrete-electrolytes, during the migration experiment. See text for details. A) R_0 and R_3; B) C_3.

and R_3 decrease steeply during the first 150 h approximately, and after that period they remain essentially constant. The value of C_3 is low and constant during the first 120 migration hours. At this time the value of the capacitance experiments a step-up to a value of about 20 μF, which is kept approximately constant up to the end of the experiment, although the values of this parameter show a considerable scatter.

The values of the dispersion factors are not shown, because most of them do not have a clear physical meaning.

3.3. Mercury intrusion porosimetry results

MIP measurements have been done on five different samples of concrete. One of them corresponds to the reference concrete, not subjected to migration. The other four samples are obtained from concrete that has been subjected to migration experiments during 410 h and 820 h. For each migration time one sample was taken from the face in contact with the catholyte, and another from the face in

Table 3
Total porosity of different concrete samples, determined using mercury intrusion porosimetry

Material	Total porosity, %
Reference concrete	7.99
410 h, anodic side	7.68
410 h, cathodic side	7.57
820 h, anodic side	8.58
820 h, cathodic side	7.03

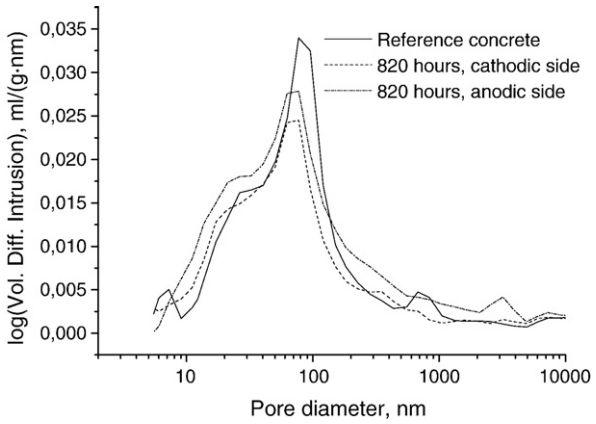

Fig. 11. Pore size distributions for some of the studied samples. Reference concrete and samples exposed to 820 h of migration test, both at the anodic and cathodic sides.

contact with the anolyte, previously freed of the deposits mentioned in Section 3.1. It seemed interesting to see if there was any variation of microstructure at both sides of the concrete samples, as previous works showed differences between the anodic and the cathodic sides [22]. The values for the total porosities measured are shown in Table 3.

Fig. 11 shows the plots of the logarithmic differential intrusion volume vs pore size, for the reference concrete, and for the samples of the anodic and cathodic sides after 820 h of migration test. For pore diameters lower than 200 nm chloride migration produces displacements of the differential intrusion curves towards the lower pore sizes. This observation points to a refinement of the capillary porosity of concrete, with a decrease of the number of large pores and an increase of the number of small pores, in agreement with previous results [22–24]. The differences, induced by migration, between the concrete microstructure at the anodic and cathodic sides, are appreciated in Fig. 11 at pore diameters higher than 200 nm. While the differential intrusion curves are rather similar for the reference concrete and the cathodic side, (only a pore family of about 0.7 μm is present in the reference curve and not appreciable in the cathodic side curve), the concrete sample at the anodic side shows higher contributions of porosity at the whole range (>200 nm), and a new pore family at about 3 μm. All these qualitative observations can be adequately quantified in Fig. 12, which shows the measured pore

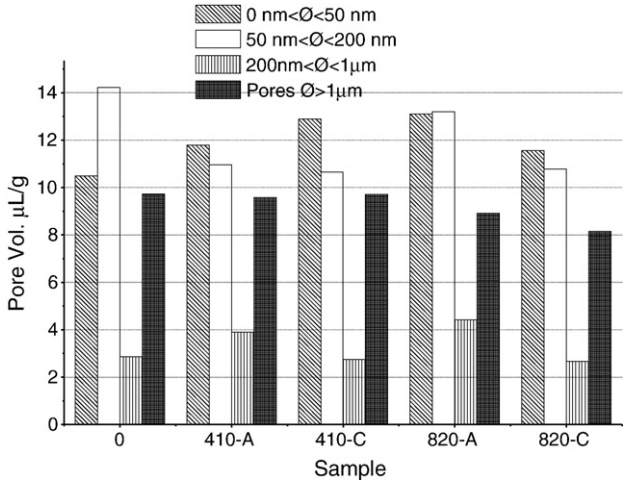

Fig. 12. Measured pore volumes at four pore diameter ranges, see text for details. The data correspond to a reference concrete sample (0), not subjected to migration, and to samples obtained after 410 and 820 h of migration for both anodic and cathodic sides.

volumes for the concrete samples, corresponding to the following pore diameter ranges: diameters lower than 50 nm (this range includes the gel pores and the finer capillary pores); diameters between 50 and 200 nm (corresponds to the mid-range capillary porosity); diameters between 0.2 and 1 μm (larger capillary pores); and diameters higher than 1 μm (coarse porosity).

As mentioned in Section 3.1, MIP measurements were also made on the materials deposited on the anodic side of the concrete samples, in order to study the possible influence they can have on the migration of chlorides through concrete. The total porosity of these materials is greater than 22%, which is much bigger than the porosity of concrete (maximum 8.58%).

4. Discussion

4.1. Modifications of the concrete microstructure during migration

The dielectric parameters representative of the microstructure of the porous material are: R_1 and R_2 (electric resistances of the percolating and occluded pores, respectively), C_1 (capacitance associated to the solid phases of the porous material), and C_2 (capacitance of the pore walls ionic double layer).

Fig. 9A shows that at the beginning of the experiment R_1 has a high value of about 6000 Ω, and during the first 100 h the value of the resistance decreases to its minimum value (180 Ω). This time coincides with the time necessary for the anolyte conductivity to start increasing (see Fig. 3A), i.e. the so-called time-lag, which has been defined before as a transient period during which porosity is filled with diffusing species [8]. The concrete samples are pre-conditioned before the migration experiment by saturation with distilled water [38]. This is the reason why at the beginning of the experiment R_1 has such a high value. While chlorides penetrate into the concrete the value of the resistance decreases, reaching a minimum value when the sample is completely saturated with chloride ions. The value of this time-lag is used to determine a very important transport property, such as the non steady-state diffusion coefficient [17]. As appreciable by comparing Figs. 3A and 9A the time-lag value can be also determined by measurements of R_1 during the migration experiments, with a precision similar to that obtained through measurements of the anolyte conductivity.

During these first 100 h, the value of R_2, associated to the non-percolating pores also decreases, from a high value, of about 1000 Ω, to some Ω, as can be seen in Fig. 9B. At the beginning of the migration experiment these pores were also saturated with distilled water, thus explaining the initial high value of R_2. As Cl^- ions saturate progressively the concrete sample, they also penetrate in the non-percolating pores, and decrease the resistivity of the electrolyte that fills these pores, parameter that is directly related to the measured resistance R_2 [45].

Fig. 9C shows the evolutions of the capacitances C_1 and C_2 through the migration experiments. During the time-lag (first 100 h) both capacitances remain at low and approximately constant values. This indicates that no appreciable changes occur in the solid fraction of concrete and at the pore walls; i.e. there is no formation of new solid phase by precipitation reactions, nor dissolution processes. This result also gives support to the idea that during the time-lag period only the inner electrolyte changes, while the solid phases remain mostly unchanged.

After finishing the time-lag period the four dielectric parameters under study in this section show growing trends, see Fig. 9. R_1 starts increasing just after finishing the time-lag, with a value of about 180 Ω at 100 h, and reaches a value of approximately 1200 Ω at the end of the experiment. R_2 starts its growing at 250 h, from a value of about 30 Ω at this time, up to a value of approximately 700 Ω, and the capacitances start their increases between 150 and 200 h, showing values of about 20 pF, and reaching final values between 100 and 250 pF. For the four parameters there is an increase of the slope of the growing lines at about 400 h.

The increases of R_1 and R_2 can be interpreted as due to a narrowing down process of the pore system during the migration experiment, i.e. a tendency to decrease the diameters of the pores, especially after the time-lag. The increase of C_1 points to the formation of new solid phases during migration. The increase of C_2 indicates that these new solid phases appear especially at the pore walls, which is also compatible with the above mentioned narrowing of the pores.

In this work MIP has been used as an auxiliary technique to confirm the results obtained using impedance spectroscopy, and their interpretation. The modifications of the differential intrusion curves, induced by 820 h of migration, point to a refinement of the capillary porosity of concrete, for pore diameters lower than 200 nm, see Fig. 11. This effect is quantified in Fig. 12. The pore volumes associated with the diameter range between 50 and 200 nm, which are about 14 μL/g for the reference concrete, are lowered to values of approximately 11 μL/g by the chloride migration treatment, except for the sample taken at the anodic side after 820 h, whose case will be discussed later. On the other hand the pore volumes corresponding to diameters lower than 50 nm, which are about 10.5 μL/g for the reference concrete, are increased to values between 11.5 and 13 μL/g by the chloride migration treatment. This result can be interpreted as a decrease of the number of mid-range capillary pores and an increase of the number of gel pores and small capillary pores, which is compatible with the results obtained by IS measurements and their interpretation, and is also in agreement with previous results [22–24].

The percentages of mercury retained after the MIP measurements, for the reference and the concrete samples taken at selected migration times, are shown in Fig. 13. The analysis of these latter data indicate that the tortuosity of the concrete pore network increases during the migration experiment, especially at the anodic side. This experimental fact gives more support to the idea of formation of new solid phases at the pore walls, as the most probable explanation for the increases of the capacitances C_1 and C_2 during the migration experiment. At this point it is interesting to look at the total porosities of the samples under study, (Table 3). The total porosity of concrete seems to decrease slightly at the cathodic side during the migration experiment, while the evolution of the porosity at the anodic side is not so clear. It is worth noting the increase of the total porosity at the anodic side after 820 migration hours, which will be discussed later. The slight porosity decrease at the cathodic side is also compatible with the refinement of the capillary porosity and formation of new solids at the pore walls during migration.

The microstructural modifications of concrete during migration, suggested by the IS analysis and confirmed by the MIP data, can be explained in terms of physical processes taking place during the passage of current. Some experimental evidence has been given that

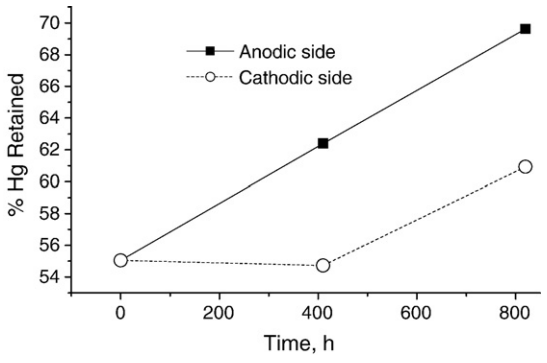

Fig. 13. Percentage of mercury retained for the five samples during the MIP measurements.

ionic migration through concrete causes partial and local decompositions of some cement hydration products: C–S–H, calcium aluminum monosulphate (AFm) [23]. Several ions can be released into the pore solution as a result of these decompositions: Ca^{2+}, OH^-, SO_4^{2-}, aluminum and silicon species. Afterwards these species, together with the migrating Cl^- ions, can participate in precipitation reactions whose products might block larger pores [23]. The formation of Friedel's salt has been observed after chloride migration experiments [21,22]. A microstructural study, [23], has shown that electrochemical Cl^- extraction treatments induced the appearance of silicon deficient reticulated C–S–H structures, formation of calcium hydroxide and calcium-aluminum-rich structures at the steel-mortar interface; and finally it was suggested that released sulphate ions migrating towards the external anode might react to produce calcium aluminum trisulphate (AFt) or gypsum. All these processes would contribute to the porosity refinement suggested by the IS measurements and observed by different techniques after chloride migration [23].

The MIP results show some differences of the pore size distributions after migration for the anodic and cathodic sides, see Fig. 11, mainly at the pore diameter ranges between 0.2 and 1 μm (larger capillary pores); and diameters higher than 1 μm (coarse porosity). This effect is quantified at Fig. 12. The pore volumes associated with the diameter range between 0.2 and 1 μm, show values of about 2.8 μL/g for the reference concrete and for the cathodic side samples after migration, while the anodic side samples show higher values of approximately 4.2 μL/g after migration. This means that the large capillary and coarse pores are almost not affected by the migration experiment, except at the anodic side, where the large capillary porosity seems to be increased. This fact is additionally confirmed by the increase of total porosity observed at the anodic side after 820 migration hours, see Table 3. In a previous study [22], it was also observed a small increase of the porosity for the anodic side, and was associated to the disturbance of the chemical equilibria or a change in the pH, because of the generation of H^+ at the anode [22]. This may cause the increase of the pore volume corresponding to the large capillary pores, and in consequence the increase of the total porosity at the anodic side. Nevertheless, in this work no apparent damage of the anodic concrete surface was observed after finishing the migration experiments.

The obtained IS results can be compared with those reported by Diaz et al. [21], during migration tests through cement mortar samples. In this latter work [21], the evolution and measured values of R_1 are in fairly good agreement with those observed here. On the other hand, the evolutions of R_2, C_1 and C_2 are a little bit different: after the initial decrease step, R_2 remains approximately constant, and the capacitances do not vary much during the migration test through mortar [21], although the measured values of these three dielectric parameters are comparable to those obtained in the present work. It is possible that the different behaviours of the dielectric parameters be due to the different nature of the porous networks of mortar and concrete. It must be taken into account that the presence of coarse aggregates in concrete gives raise to especial features, such as the interfacial transition zones between cement paste and coarse aggregates. These zones are known to have different microstructural and transport properties, as compared to bulk cement paste.

Even though the model used for the fitting of the data is quite different, some coincidences are observed with the results obtained by Loche et al. [37]. These authors also observed a decrease of the total resistance (R_1) at the initial stage of the experiment, and afterwards it remained in a value much lower than the initial one. These authors have also found an increasing tendency in the high frequency capacitance (C_1), associated to an increase in the solid phase fraction. They have also described the appearance of a low frequency loop, which has been associated to the interaction of chlorides when added to the catholyte solution [37]. This loop has not been observed in the impedance spectra corresponding to the present work, due to the different test conditions. According to the equivalent electric circuit used in the present work, the evolution of the parameters R_2 and C_2 denotes increases of the tortuosity of the pore network.

Taking into account the above considerations it is possible to conclude that the IS technique provides a means to follow sensitively the changes of the concrete microstructure during migration. From the evolutions of the dielectric parameters it is appreciable that during the initial period of the experiment the sample becomes saturated with chlorides, which can be considered a confirmation of the definition given for the time-lag period [8]. Furthermore, the changes of concrete microstructure suggested by the IS observations, i.e. a refinement of the capillary porosity of concrete due to the formation of new solid phases at the pore walls during migration, have been experimentally confirmed by MIP measurements, and are in agreement with results of previous works [22–24].

4.2. Modifications of the external electrolytes and the concrete-external electrolytes interfaces during migration

The passage of current during the chloride migration trials induces not only changes in the concrete microstructure, but also important modifications of the external electrolytes and of the concrete-external electrolytes interfaces. All these changes are reflected in the measured impedance spectra. The dielectric parameters representing the electrolytes and the external interfaces are: R_0 (resistance of the external electrolytes), R_3 (transfer resistance of the external interfaces), and C_3 (capacitance of the external interfaces).

Fig. 10A shows that the value of R_0 is high, close to 900 Ω, when starting the migration trials, and decreases rather quickly reaching a value of about 5 Ω at 150 h of migration. Afterwards the value of R_0 remains practically constant. It is appreciable from Fig. 3 that the conductivity of the catholyte is always greater than the conductivity of the anolyte. This means that the main contribution to R_0 is the electric resistance of the anolyte, especially at the beginning of the migration experiments (first 100 h). The variation of the anolyte conductivity during the first 100 h of migration is not appreciable due to the scale used in Fig. 3A, but it increases from an initial value of approximately 50 μS/cm, (typical value of distilled water), to a value close to 1 mS/cm, at the end of the time-lag period (100 h in this case), and reaches a value of 10 mS/cm at 150 h. This increase is due to the leaching and migration of ions, mainly OH^- and Cl^-, from the concrete sample to the anolyte, and also to the ionic products of the incipient anodic reactions [11]. Fig. 14 shows the almost linear relationship found, (correlation coefficient r=0.93), between the calculated value of the electrolyte resistance, R_0, obtained by fitting the impedance spectra to the

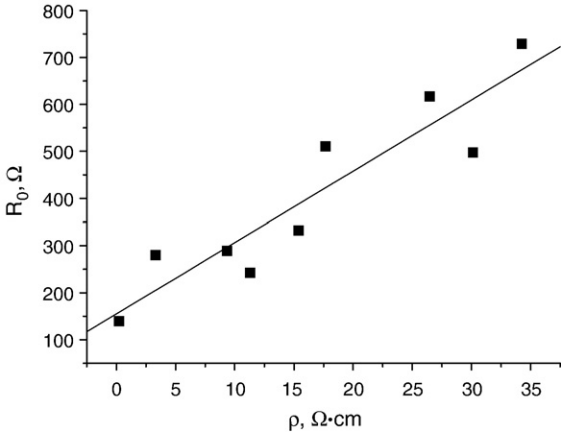

Fig. 14. Relationship between the electrolyte resistance, R_0, determined by fitting the IS spectra, and the anolyte resistivity (ρ). The best linear fit for the experimental data corresponds to the expression: $R_0 = 15.14 \cdot \rho + 154.98$ (correlation coefficient r=0.93).

equivalent circuit, and the electric resistivity of the anolyte, calculated as the inverse of the measured conductivity.

The evolution of R_3 and C_3 also has interest, and should reflect the changes at the concrete-external electrolytes interfaces. These dielectric parameters were firstly introduced in a recent paper [21]. It must be recalled that, during the migration experiments, deposits were formed on the cement paste surface at the anodic side of concrete, see Section 3.1. Fig. 10A shows that the initial value of R_3 is high (about 2400 Ω), and decreases rather quickly during the first 100 h of migration (the time-lag period), showing afterwards a practically constant value of about 20 Ω. The high initial value of the transfer resistance at the external interfaces can be due to the high resistance of the concrete sample, because it was saturated with distilled water prior to the migration experiment, and to the initial absence of ions at the anolyte (distilled water). The progressive saturation of the concrete sample with chlorides and the progressive increase of the anolyte conductivity makes easier the ionic transfer between sample and anolyte, and as a consequence, the resistance of the interface will decrease. It is worth noting that the value of R_3 never increases during the migration trial, as can be seen in Fig. 10A, even though solid deposits were formed at the anodic side of the concrete sample. This suggests that these deposits do not hinder the ionic transfer through the concrete-external electrolyte interface.

To check if there was some kind of reaction between corrosion products of the electrodes, solutions, and concrete, SEM was used to obtain elementary compositions of the deposits formed at the anodic side of the concrete samples after 410 and 820 h of migration test, see Table 2. The most abundant elements in these deposits are oxygen, and the metals constituting the stainless steel electrodes (Fe, Cr and Ni), while Ca and Al appear only after 820 h of migration and in a quantity lower than 0.5%. This implies there are no products of reaction with cement paste in these solids. Taking into account the compositions of the deposited layers on the concrete surface in contact with the anolyte, and the spatial distribution of the deposits, (they appear over the exposed cement paste and not over the aggregates), it is possible to state that these layers are formed by interaction of the metallic cations (Fe^{3+}, Cr^{3+}, Ni^{2+}) coming from the electrochemical dissolution of the anode, and hydroxide ions migrating from the cement paste. It is interesting to recall that the anodic electrochemical reactions lead to a decrease of the pH [11,22], and the acid character of the anolyte may hinder the precipitation of these hydroxides or oxides in the bulk anolyte solution, but they can easily be formed at the OH^- ions source, which is clearly identified here at the cement paste surface. The total porosity of these deposits was measured giving a minimum porosity of 22%, much higher than the porosity of concrete.

The only parameter which seems to be affected by the deposition of oxides at the anodic side of the concrete sample is the capacitance C_3, as can be appreciated in Fig. 10B. The value of this capacitance is very low and approximately constant until 120 h of migration. At this time, which represents approximately the duration of the time-lag, the value of C_3 experiments an increase to a value of about 20 μF. Afterwards the value of C_3 shows an important scatter, but its mean value is kept approximately equal to 20 μF. It is likely that the formation of the oxide deposits at the anodic side of concrete takes place mainly after finishing the time-lag period, due to an increase of the ionic transfer across the concrete-anolyte interface, which in turn is due to the increase of the current intensity passing through the concrete sample, as suggested by the evolution of the potential drop across the concrete sample during the migration trial, see Fig. 4. The appearance of the deposits at the concrete anodic face would increase the active surface of the interface, and consequently the value of the capacitance C_3.

The evolutions of R_0, R_3 and C_3 found in this work are quite different to those reported by Diaz et al. [21] during migration experiments performed with cement mortar samples. These authors observed a practically constant value of R_0, an increasing trend for R_3 (steeper at the beginning), and a steady increasing trend for C_3, during their migration trials. Nevertheless these differences can be adequately explained by considering the different conditions and experimental setups used, as compared with those used in this work. In the abovementioned work [21] the initial anolyte was a 0.01 M NaOH solution and graphite sheets were used for applying the driving electric field. The high initial conductivity of the 0.01 M NaOH solution explains the constancy of R_0 during migration in Ref. [21]. The nature of the driving electrodes used by Diaz et al. (graphite) explain why they did not observe the formation of deposits with the colour of Fe oxides at the anodic surface of their mortar samples. Instead, they reported the appearance of a precipitate of powdery nature on mortar at the anolyte interface [21], which seems to have hindered considerably the ionic transfer through the concrete-anolyte interface, since R_3 increased from an initial value of 10^2 Ω to a value of about 10^3 Ω when finishing the migration. The capacitance C_3 also shows a very important increase from an initial value of about 1 μF to a final value higher than 10^3 μF at the end of the migration experiments through mortar [21], a much higher value than that found for C_3 in this work (about 20 μF). Furthermore, the precipitate formed on the anodic face of mortar is related to the damage of the mortar's skin due to the acidity produced by the electrochemical anodic reactions [21], i.e. it is most likely produced by reaction of the acid anolyte with the cement paste at the mortar surface; while the deposits observed in this work are not due to reaction with concrete. It must be taken into account that when using a graphite anode for the migration experiment a higher acidity is produced, as compared with the case of a steel anode. In the case of a steel electrode part of the electric charge exchanged is carried by electrochemical dissolution of the anode with releasing of metallic ions and production of a lower quantity of H^+ ions. The acidification of the anolyte is also likely to be higher in the case of mortar samples, in comparison with concrete samples, because the higher porosity of mortar allows the passage of higher current densities for the same feeding voltage (12 V).

All these facts indicate that the IS technique and the equivalent circuit used to model the dielectric response of the system, are able to follow the main changes of the external electrolytes and of the concrete-external electrolytes interfaces during a migration experiment. Furthermore, the dielectric response seems to be also sensitive to variations of the experimental conditions.

The IS technique presents some specific features which make it very attractive for studies of the modifications of concrete microstructure during migration, as compared with other microstructural techniques, such as PIM, SEM or X-ray diffraction (XRD). IS measurements are non-destructive, which allows to follow the changes at different times during the experiment with no perturbation or damage of the sample. The second important advantage of impedance spectroscopy is that the measurement is global, i.e. it reflects the contribution of the whole sample, while for the other techniques the measurements are local, and thus strongly dependent on the part of the concrete studied, and on the representativity of the samples. Local techniques, such as PIM or SEM are useful for detecting differences induced by migration, for instance between anodic and cathodic sides of the sample. But it is difficult with these results to get an idea on how these local changes affect the transport properties of the whole sample. Such a global idea can be better obtained through IS measurements, that reflect the mean behaviour of the whole sample. For instance in this work it is made clear that the local increases of the large capillary porosity at the anodic side of concrete during migration do not affect significantly the transport properties, since the growing trend of R_1 during the second part of the experiment is never reduced, and the value of the resistance R_3 is also approximately constant during this last part of the migration test. This suggests that the damage of the concrete at the anodic side, due to increasing acidity of the anolyte, is localized at the surface, and most probably it does not

induce an increase of the chloride permeability of concrete, at least in the experimental conditions of this work.

5. Conclusions

All the previous results can be summarized in the following conclusions:

a) The technique of impedance spectroscopy, and the equivalent circuit used to model the dielectric response of the system, allow to follow sensitively the changes of the concrete microstructure, and those taking place at the external electrolytes and interfaces, during an ionic migration experiment.
b) The evolutions of the dielectric parameters suggest that during the initial part of the migration test, and with the experimental conditions of this work, the concrete sample becomes saturated with chlorides, which represents a confirmation of the definition of the time-lag period.
c) The variations of the dielectric parameters during the migration test can be interpreted in the following terms: the pore network experiments a narrowing down process, i.e. there is a tendency to decrease the diameters of the pores, and this is due to the formation of new solid phases at the pore walls. These interpretations are confirmed experimentally by mercury intrusion porosimetry results.
d) The dielectric response of the whole migration cell is sensitive to variations of the experimental conditions, i.e. use of different electrodes for establishing the electric field, or changes of the composition of the initial external electrolytes. When using stainless steel driving electrodes oxide and hydroxide deposits are formed at the anodic side of the concrete sample, which do not modify the transport properties of concrete.

Acknowledgements

We thank the funding received for this research from the Generalitat Valenciana through project GV05/196, and from the Ministerio de Educación y Ciencia of Spain and Fondo Europeo de Desarrollo Regional (FEDER) through project BIA2006-05961. Dr Isidro Sánchez is indebted to the Spanish Ministry of Education and Science for a fellowship corresponding to the "Juan de la Cierva" programme. We would like to thank Prof. C. Andrade and Dr. M. Castellote of the Eduardo Torroja Institute of Construction Sciences (CSIC, Spain) for advice and valuable comments on the chloride migration test methodology.

References

[1] C. Alonso, C. Andrade, M. Izquierdo, X.R. Nóvoa, M.C. Pérez, Effect of protective oxide scales in the macrogalvanic behaviour of concrete reinforcements, Corros. Sci. 40 (1998) 1379–1389.
[2] C. Andrade, M. Keddam, X.R. Nóvoa, M.C. Pérez, C.M. Rangel, H. Takenouti, Eletrochemical behaviour of steel rebars in concrete: influence of environmental factors and cement chemistry, Electrochim. Acta 46 (2001) 3905–3912.
[3] A.K. Suryavanshi, J.D. Scantlebury, S.B. Lyon, Pore size distribution of OPC & SRPC mortars in presence of chlorides, Cem. Concr. Res. 25 (5) (1995) 980–988.
[4] M. Cabeza, M. Franco, M. Izquierdo, X.R. Nóvoa, I. Sánchez, Effect des chlorures sur les propietes chimiques et barriere de la pâte de ciment portland, 13eme Forum sur les Impedances Electrochimiques, Paris, 2000.
[5] M. Collepardi, A. Marcialis, R. Turriziani, Penetration of chloride ions in cement pastes and in concretes, J. Am. Ceram. Soc. 55 (1972) 534–535.
[6] C.L. Page, N.R. Short, A. El-Tarras, Diffusion of chloride ions in hardened cement pastes, Cem. Concr. Res. 11 (1981) 395–406.
[7] S. Goto, D.M. Roy, Diffusion of ions through hardened cement paste, Cem. Concr. Res. 11 (1981) 751–757.
[8] A. Atkinson, A.K. Nickerson, The diffusion of ions through water-saturated cement, J. Mater. Sci. 19 (1984) 3068–3078.
[9] D. Whiting, Rapid measurements of the chloride permeability of concrete, Public Roads 45 (1981) 101–112.
[10] L. Tang, L.O. Nilsson, Rapid determination of the chloride diffusivity in concrete by applying an electric field, ACI Mater. J. 89 (1) (1992) 49–53.
[11] C. Andrade, Calculation of chloride diffusion coefficients in concrete from ionic migration measurements, Cem. Concr. Res. 23 (1993) 724–742.
[12] T. Zhang, O.E. Gjørv, An electrochemical method for accelerated testing of chloride diffusivity in concrete, Cem. Concr. Res. 24 (8) (1994) 1534–1548.
[13] P.E. Streicher, M.G. Alexander, A chloride conduction test for concrete, Cem. Concr. Res. 25 (6) (1995) 1284–1294.
[14] A. Delagrave, J. Marchand, E. Samson, Prediction of diffusion coefficients in cement based materials on the basis of migration experiments, Cem. Concr. Res. 26 (12) (1996) 1831–1842.
[15] J.M. Frederiksen, H.E. Sørensen, A. Andersen, O. Klinghoffer, The effect of the w/c ratio on chloride transport into concrete — immersion, migration and resistivity tests, in: J.M. Frederiksen (Ed.), HETEK report, Danish Road Directorate, 1997.
[16] O. Truc, J.P. Ollivier, M. Carcassès, A new way for determining the chloride diffusion coefficient in concrete from steady state migration tests, Cem. Concr. Res. 30 (2) (2000) 217–226.
[17] M. Castellote, C. Andrade, C. Alonso, Measurements of the steady and non-steady-state chloride diffusion coefficients in a migration test by means of monitoring the conductivity in the anolyte chamber. Comparison with natural diffusion tests, Cem. Concr. Res. 31 (10) (2001) 1411–1420.
[18] M.A. Climent, G. de Vera, J.F. Lopez, E. Viqueira, C. Andrade, A test method for measuring chloride diffusion coefficients through nonsaturated concrete. Part I. The instantaneous plane source diffusion case, Cem. Concr. Res. 32 (2002) 1113–1123.
[19] Chlortest Project, www.chlortest.org.
[20] M. Shi, Z. Chen, J. Sun, Determination of chloride diffusivity in concrete by AC impedance spectroscopy, Cem. Concr. Res. 29 (1999) 1111–1115.
[21] B. Díaz, X.R. Nóvoa, M.C. Pérez, Study of the chloride diffusion in mortar: a new method of determining diffusion coefficients based on impedance measurements, Cem. Concr. Compos. 28 (3) (2006) 237–245.
[22] M. Castellote, C. Andrade, C. Alonso, Changes in concrete pore size distribution due to electrochemical chloride migration trials, ACI Mater. J. 96 (3) (1999) 314–319.
[23] T.D. Marcotte, C.M. Hansson, B.B. Hope, The effect of the electrochyemical chloride extraction treatment on steel-reinforced mortar. Part II. Microstructural characterization, Cem. Concr. Res. 29 (1999) 1561–1568.
[24] M. Siegwart, J.F. Lyness, B.J. McFarland, Change of pore size in concrete due to electrochemical chloride extraction and possible implications for the migration of ions, Cem. Concr. Res. 33 (2003) 1211–1221.
[25] W.J. McCarter, R. Brousseau, The a.c. response of hardened cement paste, Cem. Concr. Res. 20 (1990) 891–900.
[26] P. Gu, P. Xie, Y. Fu, J.J. Beaudoin, A.C. impedance phenomena in hydrating cement systems: frequency dispersion angle and pore size distribution, Cem. Concr. Res. 24 (1994) 86–88.
[27] I. Sánchez, Aplicación de la espectroscopía de impedancia a la determinación de la microestructura y propiedades mecánicas de la pasta y mortero de cemento Pórtland. PhD Thesis, (only available in Spanish), Universidade de Vigo, Spain (2002).
[28] C. Andrade, L. Soler, X.R. Nóvoa, Advances in electrochemical impedance measurements in reinforced concrete, Mater. Sci. Forum 192–14 (1995) 843–856.
[29] B.J. Christensen, R.T. Coverdale, R.A. Olson, S.J. Ford, E.J. Garboczi, H.M. Jennings, T.O. Mason, Impedance spectroscopy of hydrating cement-based materials: measurement, interpretation and application, J. Am. Ceram. Soc. 77 (1994) 2789–2804.
[30] R.T. Coverdale, B.J. Christensen, T.O. Mason, H.M. Jennings, E.J. Garboczi, Interpretation of the impedance spectroscopy of cement paste via computer modelling: Part II. Dielectric response, J. Mater. Sci. 29 (1994) 4984–4992.
[31] R.A. Olson, B.J. Christensen, R.T. Coverdale, S.J. Ford, G.M. Moss, H.M. Jennings, T.O. Mason, E.J. Garboczi, Interpretation of the impedance spectroscopy of cement paste via computer modelling: Part I. Bulk conductivity and offset resistance, J. Mater. Sci. 30 (1995) 712–719.
[32] R.A. Olson, B.J. Christensen, R.T. Coverdale, S.J. Ford, G.M. Moss, H.M. Jennings, T.O. Mason, E.J. Garboczi, Interpretation of the impedance spectroscopy of cement paste via computer modelling: Part III. Microstructural analysis of frozen cement paste, J. Mater. Sci. 30 (1995) 5078–5086.
[33] M. Keddam, H. Takenouti, X.R. Nóvoa, C. Andrade, C. Alonso, Impedance measurements on cement paste, Cem. Concr. Res. 27 (1997) 1191–1201.
[34] C. Andrade, V.M. Blanco, A. Collazo, M. Keddam, X.R. Nóvoa, H. Takenouti, Cement paste hardening process studied by impedance spectroscopy, Electrochim. Acta 44 (1999) 4313–4318.
[35] Z. Stoynov, Z.D. Vladikova, P. Zoltowski, E. Makowska, Selectivity study of the differential impedance analysis — comparison with the non-linear least-squares method, Electrochim. Acta 47 (2002) 2943–2951.
[36] M. Cabeza, P. Merino, A. Miranda, X.R. Nóvoa, I. Sánchez, Impedance spectroscopy study of hardened portland cement paste, Cem. Concr. Res. 32 (2002) 881–891.
[37] J.M. Loche, A. Ammar, P. Dumargue, Influence of the migration of chloride ions on the electrochemical impedance spectroscopy of mortar paste, Cem. Concr. Res. 35 (2005) 1797–1803.
[38] ASTM Standard C 1202-97, Standard test method for electrical indication of concrete's ability to resist chloride ion penetration, Annual Book of ASTM Standard Section 4, vol. 04.02, 2000.
[39] E. Barsoukov, J.R. McDonald, Impedance spectroscopy, Theory, Experiments, and Applications, 2nd Ed., Wiley Interscience, New Jersey, USA, 2005, p. 149.
[40] C. Alonso, C. Andrade, X.R. Nóvoa, M. Keddam, H. Takenouti, Study of the dielectric characteristics of cement paste, Mater. Sci. Forum 289–292 (1998) 15–28.
[41] S. Diamond, Aspects of concrete porosity revisited, Cem. Concr. Res. 29 (1999) 1181–1188.
[42] S. Diamond, Mercury porosimetry. An inappropriate method for the measurement of pore size distributions in cement-based materials, Cem. Concr. Res. 30 (2000) 1517–1525.

[43] C. Galle, Effect of drying on cement-based materials pore structure as identified by mercury intrusion porosimetry. A comparative study between oven-, vacuum-, and freeze drying, Cem. Concr. Res. 31 (2001) 1467–1477.
[44] R. Kumar, B. Bhattacharjee, Study on some factors affecting the results in the use of MIP method in concrete research, Cem. Concr. Res. 33 (2003) 417–424.
[45] M. Cabeza, M. Keddam, X.R. Nóvoa, I. Sánchez, H. Takenouti, Impedance spectroscopy to characterize the pore structure during the hardening process of Portland cement paste, Electrochim. Acta 51 (2006) 1831–1841.
[46] P. Pedeferri, L. Bertolini, La durabilità del calcestruzzo armado, Mc Graw Hill, Milan, 2000.
[47] G. de Vera, A. Hidalgo, M.A. Climent, C. Andrade, C. Alonso, Chloride-ion activities in simplified synthetic concrete pore solutions: the effect of accompanying ions, J. Am. Ceram. Soc. 83 (3) (2000) 640–644.